







# A congenital hydrocephalus-causing mutation in Trim71 induces stem cell defects via inhibiting *Lsd1* mRNA translation

Qiuying Liu<sup>1</sup> , Mariah K Novak<sup>1</sup> , Rachel M Pepin<sup>1</sup> , Katharine R Maschhoff<sup>1</sup> , Kailey Worner<sup>1</sup>, Xiaoli Chen<sup>2</sup>, Shaojie Zhang<sup>2</sup>  & Wenqian Hu<sup>1,\*</sup> 

## Abstract

**Congenital hydrocephalus (CH) is a major cause of childhood morbidity. Mono-allelic mutations in Trim71, a conserved stem-cell-specific RNA-binding protein, cause CH; however, the molecular basis for pathogenesis mediated by these mutations remains unknown. Here, using mouse embryonic stem cells as a model, we reveal that the mouse R783H mutation (R796H in human) alters Trim71's mRNA substrate specificity and leads to accelerated stem-cell differentiation and neural lineage commitment. Mutant Trim71, but not wild-type Trim71, binds *Lsd1* (*Kdm1a*) mRNA and represses its translation. Specific inhibition of this repression or a slight increase of *Lsd1* in the mutant cells alleviates the defects in stem cell differentiation and neural lineage commitment. These results determine a functionally relevant target of the CH-causing Trim71 mutant that can potentially be a therapeutic target and provide molecular mechanistic insights into the pathogenesis of this disease.**

**Keywords** congenital hydrocephalus; embryonic stem cell; *Lsd1*; RNA-binding protein; Trim71

**Subject Categories** RNA Biology; Stem Cells & Regenerative Medicine; Translation & Protein Quality

**DOI** 10.15252/embr.202255843 | Received 22 July 2022 | Revised 3 December 2022 | Accepted 7 December 2022 | Published online 27 December 2022

**EMBO Reports (2023) 24: e55843**

## Introduction

RNA-binding proteins (RBPs) control mRNA fate and are critical regulators of gene expression (Glisovic *et al.*, 2008). These proteins play essential roles in animal development, and aberrations in RBPs contribute to a wide variety of human diseases (Lukong *et al.*, 2008; Brinegar & Cooper, 2016; Gebauer *et al.*, 2021). While the details of RBP-mediated regulations in a diverse range of physiological processes are becoming increasingly clear, our understanding of the

molecular mechanisms by which mutations in RBPs result in diseases is still limited.

Congenital hydrocephalus (CH), a significant cause of childhood morbidity, is caused by imbalanced neurogenesis that leads to abnormal accumulation of cerebrospinal fluid in brain ventricles (Kahle *et al.*, 2016). The primary treatment for CH is neurosurgical shunting, which has numerous complications. Human whole-exome sequencing studies and pedigree analysis have identified several CH-causing mutations, including two mono-allelic and potential gain-of-function missense mutations in Trim71 (Furey *et al.*, 2018; Jin *et al.*, 2020), a stem-cell specific RBP that is highly conserved from *Caenorhabditis elegans* to human (Ecsedi & Grosshans, 2013; Connacher & Goldstrohm, 2021). Trim71 binds to target mRNAs and downregulates their expression through translational repression and/or enhanced mRNA degradation (Chang *et al.*, 2012; Loedige *et al.*, 2013; Worringer *et al.*, 2014; Aeschmann *et al.*, 2017; Welte *et al.*, 2019; Liu *et al.*, 2021a). Genetic studies in mice indicate that Trim71 is essential for early embryogenesis and proper neural differentiation, indicating it has critical functions during normal development (Maller Schulman *et al.*, 2008; Chen *et al.*, 2012; Cuevas *et al.*, 2015). Mice with the homologous human CH-causing point mutations in Trim71 also have CH and display defects in neurogenesis (Duy *et al.*, 2022), arguing for conserved mechanisms of pathogenesis from the Trim71 mutants. Although these animal studies revealed the developmental defects from the Trim71 mutants, our understanding of the molecular mechanisms by which these pathogenic mutations in Trim71 lead to cellular defects is still very limited.

Here, we dissected the molecular mechanisms of pathogenesis mediated by a disease-causing mutation in Trim71. Using mouse embryonic stem cells (mESCs) as a model, we compared the transcriptome-wide targets of wide-type (WT) Trim71 and the Trim71 bearing a homologous human CH-causing mutation (R783H in mouse, which is equivalent to R796H in human). This mutation significantly alters Trim71's mRNA substrates and leads to accelerated stem cell differentiation and neural lineage commitment. Among the mRNAs that are uniquely bound by the mutant Trim71,

<sup>1</sup> Department of Biochemistry and Molecular Biology, Mayo Clinic, Rochester, MN, USA

<sup>2</sup> Department of Computer Science, University of Central Florida, Orlando, FL, USA

\*Corresponding author. Tel: +1 507 284 2133; E-mail: hu.wenqian@mayo.edu

we determined that the mutant Trim71 represses *Lsd1* (*Kdm1a*) mRNA translation. Specific inhibition of this repression through deleting the mutant Trim71's binding site in the 3'UTR of *Lsd1* mRNA or a modest increase of *Lsd1* in the mutant mESCs alleviates the defects in stem cell differentiation and neural lineage commitment. Altogether, these results determine a functionally relevant target of the CH-causing Trim71 mutant that can potentially be a therapeutic target and provide molecular mechanistic insights into the pathogenesis of CH caused by the R796H mutation in *TRIM71*. Moreover, our finding revealed that a disease-causing mutation in an RBP does not abolish RNA binding but alters its binding specificity, a mechanism by which gain-of-function mutations in RBPs can result in disease.

## Results

### R783H Trim71 causes stem-cell and neural-differentiation defects

We used mESCs as a model to study the CH-causing mutations in Trim71 because: (i) Trim71 is a highly conserved stem-cell-specific RBP (Ecsedi & Grosshans, 2013; Connacher & Goldstrohm, 2021); (ii) the homologous human CH-causing point mutations in mouse Trim71 also lead to CH and neurogenesis defects (Duy et al, 2022). We chose the FLAG-Trim71 mESCs for mechanistic studies, because the bi-allelic FLAG-tag knock-in at the N-terminus of Trim71 in these mESCs enables unambiguous detection and isolation of the endogenous Trim71 using an anti-FLAG monoclonal antibody (Liu et al, 2021a). Here, we studied the R783H Trim71 mutation in mouse, which is equivalent to the CH-causing R796H mutation in human TRIM71 (Furey et al, 2018; Jin et al, 2020). This mutation is within the RNA-binding domain of Trim71 (Fig EV1A), suggesting an alteration of the interactions between Trim71 and its target RNAs.

Using genome editing, we generated both mono-allelic and bi-allelic R783H mutations on Trim71 in the FLAG-Trim71 mESCs (Fig EV1B). In human, the mono-allelic R796H mutation in TRIM71 causes CH, arguing that this mutation can be a gain-of-function mutation (Furey et al, 2018; Jin et al, 2020). A challenge of

mechanistic studies in the heterozygous background, however, is that it is difficult to discriminate whether the identified phenotypes/interactions (e.g., mRNA substrates) are mediated directly by the mutant protein or by the potential alterations of the WT protein (e.g., potential dimerization between WT and mutant proteins). To circumvent this, we first used mESCs with the bi-allelic mutation for functional and mechanistic studies on the R783H Trim71 mutant, and then we examined whether the identified mechanistic insights are disease relevant in mESCs with the mono-allelic R783H mutation in Trim71.

The R783H mutation, in either the homozygous or the heterozygous background, does not alter the proliferation and apoptosis of mESCs under both stemness and differentiating conditions (Fig EV2A–D). By contrast, the Trim71 knockout (KO) mESCs displayed impaired growth and increased apoptosis (Fig EV2A–D), which is consistent with the previous report (Chang et al, 2012). These results argue that the R783H is not a loss-of-function mutation. Moreover, the R783H mutation does not impact the microRNA pathway in mESCs, because neither the levels of Ago2, the major argonaute protein in mESCs (Liu et al, 2021b), nor a group of microRNAs involved in either differentiation (e.g., let-7 microRNAs) or pluripotency (e.g., the miR-290, 291, 293) are altered in the R783H mutant mESCs (Appendix Fig S1).

In mESCs with the bi-allelic mutation, the R783H mutation resulted in a modest decrease (~80% of WT levels) in Trim71 levels (Fig 1A) but did not impact stem cell self-renewal, as revealed by either examining the expression of pluripotency factors (Fig 1A) or colony formation assays (Fig 1B). However, when subjected to the exit pluripotency assay, which evaluates the rate mESCs exit the pluripotent state (Betschinger et al, 2013), the R783H mutant mESCs lost pluripotency at a significantly increased rate compared to either the WT or the Trim71 knockout mESCs (Fig 1C). Moreover, when subjected to differentiation via embryonic body (EB) formation for 5 days, the R783H mutant mESCs showed decreased levels of pluripotency factors than either the WT or Trim71 knockout mESCs (Fig 1D). Consistent with these findings, immunofluorescence staining revealed that differentiating R783H mutant mESCs had less Rex1, a marker of pluripotency, than either the WT or the Trim71 KO mESCs (Fig 1E and F). These results collectively indicate that the R783H mutant mESCs are more prone to differentiation and

**Figure 1. CH-causing Trim71 mutation results in stem cell and neural differentiation defects in mESCs.**

- A Western blotting in the WT, Trim71 knockout (Trim71\_KO), and the Trim71 mutant (R783H) mESCs. The signals from the pluripotency factors Nanog and Oct4 were obtained through short (~10 s) exposure.
- B Colony formation assay for mESCs. The mESCs were cultured in 15% FBS + Lif for 7 days, and the resultant colonies were fixed and stained for AP.
- C Exit pluripotency assay for mESCs. The mESCs were induced to exit pluripotency in medium without Lif for 2 days and then switched to 2i + Lif medium for 5 days. The resultant colonies were fixed and stained for AP.
- D Western blotting of pluripotency factors during EB formation. The signals from the pluripotency factors Nanog and Oct4 were obtained through long (5–10 min) exposure.
- E Immunofluorescence (IF) staining showing the expression level of Rex1 in mESCs cultured in the stemness (2i + Lif) and differentiating (15% FBS – Lif) conditions.
- F Relative intensity of IF signals from individual cells in experiment associated with (E). The results represent the means ( $\pm$ SD) of three independent IF stainings.
- G Expression of neural lineage markers during mESCs neural differentiation.
- H Relative intensity of Pax6 and Sox1 at the Day 5 in (G). The results represent the means ( $\pm$ SD) of three independent measurements.
- I IF staining of Nestin. The quantifications represent the means ( $\pm$ SD) of three independent experiments.

Data information: In (A, D, and G), representative Western blots are shown, and the quantifications represent the means ( $\pm$ SD) of three independent experiments. In (B and C), the colony morphology and AP intensity were evaluated through microscopy. 100–200 colonies were examined each time to determine the percentage of undifferentiated colonies. The results represent the means ( $\pm$ SD) of three independent experiments. One-Way ANOVA was used to determine the significance of the difference, \* $P < 0.05$ ; and n.s., not significant ( $P > 0.05$ ).

Source data are available online for this figure.

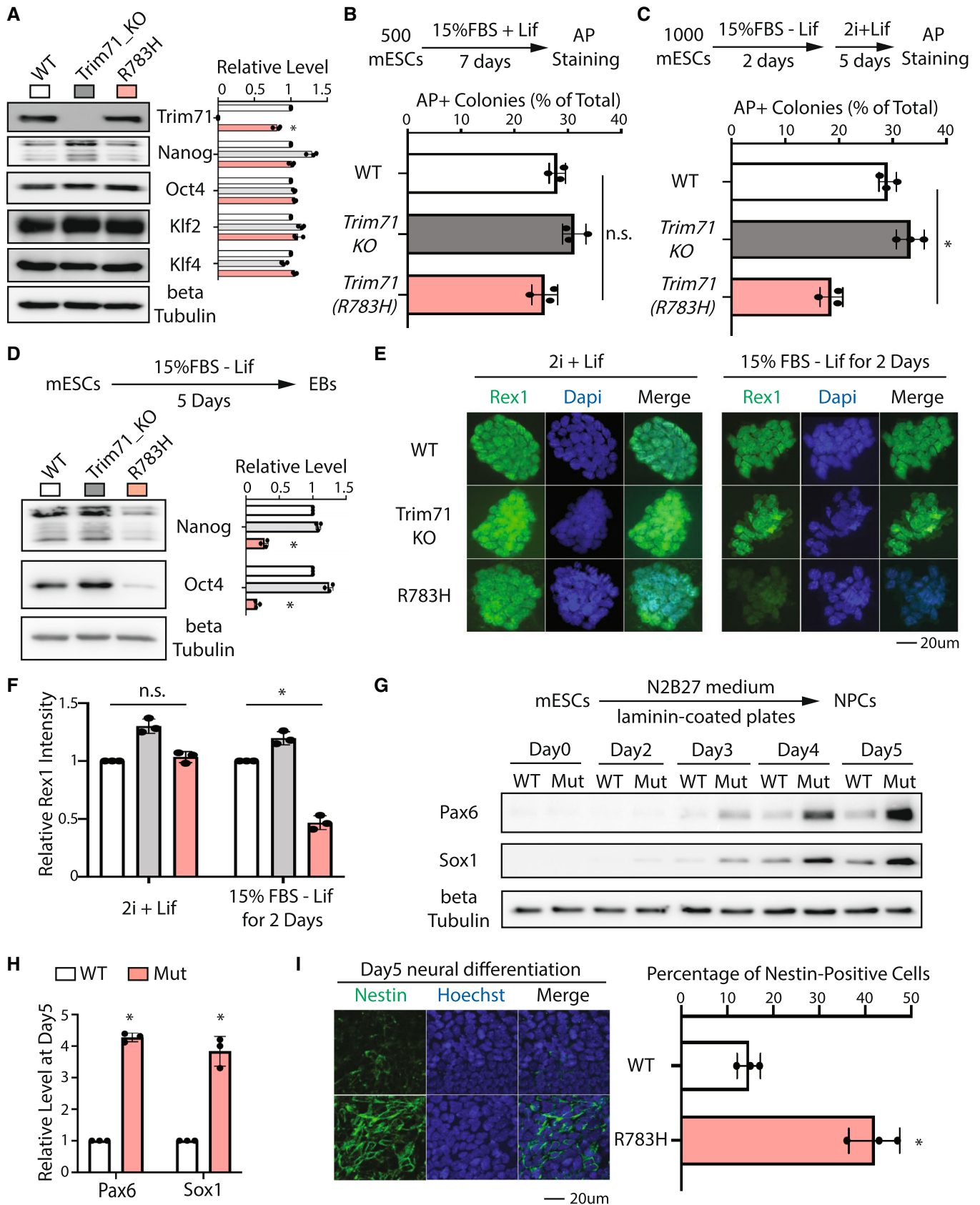


Figure 1.

argue that the R783H Trim71 mutation is a gain-of-function mutation, which is consistent with the observations that mono-allelic R796H mutation in TRIM71 results in CH (Furey et al, 2018).

As CH is a neurological disorder (Kahle et al, 2016), we subjected mESCs to monolayer neural differentiation (Mulas et al, 2019) and monitored the appearance of neural progenitor cells by examining the expression of Sox1 and Pax6, two critical transcription factors essential for neuroectodermal specification in mammals (Li et al, 2005). Compared to the WT mESCs, R783H mESCs showed both the earlier appearance and increased immunoblotting intensity of these two factors during the neural differentiation (Fig 1G and H), indicating that the CH-causing R783H Trim71 mutation resulted in accelerated neural differentiation in mESCs. Consistently, immunofluorescence staining of Nestin, a marker of neural progenitor cells, indicated the R783H cells express higher Nestin than the WT cells at the Day 5 of neural differentiation (Fig 1I). Moreover, when subjected to spontaneous differentiation through EB formation, the R783H mESCs specifically expressed more ectoderm markers than the WT mESCs (Appendix Fig S2). Altogether, these results indicated that the R783H Trim71 mutant led to stem cell and neural differentiation defects in mESCs.

### R783H Trim71 has altered target mRNA binding

The R783H mutation is located in the RNA-binding domain of Trim71 (Fig EV1A). To determine how this mutation impacts Trim71:RNA interactions, we identified transcriptome-wide targets of the R783H Trim71 mutant in mESCs using crosslinking immunoprecipitation and sequencing (CLIP-seq; Fig 2A; Darnell, 2010), which also revealed the R783H Trim71 binding region(s) on the target mRNAs. CLIP-seq was performed on the mESCs grown in the 2i + lif medium, which suppresses differentiation and maintains mESCs in the ground state (Ying et al, 2008). These culture conditions eliminated the potential differentiation differences between the WT and the R783H mESCs (Appendix Fig S3) and enabled us to evaluate how the CH-causing mutation impacts Trim71's target recognition under the same developmental state.

Comparative analysis of the CLIP-seq data from R783H Trim71 and WT Trim71 (Liu et al, 2021a) revealed two similarities. First, 3'UTR is one of the major binding regions for both the WT and the mutant Trim71 (Fig 2B and Dataset EV1). Second, WT and mutant-binding sites have a similar over-representation of predicted stem-loop structures, but no enriched primary sequence motifs, compared with randomized sequences, consistent with the results from *in vitro* studies that Trim71 recognizes structural motifs (Kumari et al, 2018; Fig 2C). Despite these common features, there is only a

small overlap between the mRNAs bound by WT Trim71 and the mutant Trim71 (Fig 2D), implying that the mutant Trim71 regulates a different set of mRNAs compared to WT Trim71 does. To validate this finding, we performed CLIP-qRT-PCR in WT and the mutant mESCs. Both WT and the mutant Trim71 bound *Cdkn1a* mRNA, a common target identified in the CLIP-seq data; however, only the mutant Trim71 bound *Lsd1*, *Ddx6*, and *Trim25* mRNAs (Fig 2E), three of the mutant-specific targets identified in the CLIP-seq data. Altogether, these results indicated that the CH-causing mutation in Trim71 significantly alters the substrate mRNAs to which it binds.

To determine whether or not this alteration of substrate RNAs is due to difference of RNA availability, we surveyed the transcriptomes of the WT and the R783H mutant mESCs grown in the 2i + lif medium (Fig EV3A), where both of these two types of mESCs have the same developmental status (Appendix Fig S3). Most (541 of 545) of the R783H Trim71 mutant's target RNAs were not differentially expressed between the WT and the R783H mESCs (Fig EV3B–D), indicating that the difference of substrate RNAs between the WT and the R783H mutant Trim71 is not caused by the RNA availability in the WT and the R783H mESCs. Moreover, this result also argues that the R783H Trim71 mutant does not destabilize its substrate RNAs.

Although the WT Trim71 and the R783H Trim71 bind two sets of different mRNAs, gene ontology each of these two sets of mRNAs were over-represented for the genes involved in regulating stem cell differentiation and pluripotency (Fig 2F). This observation is consistent with the finding that the R783H Trim71 mutant mESCs displayed stem cell and neural differentiation defects (Fig 1). A caveat in interpreting these results is that binding does not necessarily result in expression changes. To identify the functional targets of the R783H Trim71 mutant, we used the following criteria (Fig 3A): (i) mRNAs uniquely bound by the mutant Trim71 but not the WT Trim71; (ii) mRNAs encoding proteins with conserved functions in controlling stem cell differentiation; (iii) mRNAs abundantly expressed in mESCs. Western blotting on the resulting candidates revealed that *Lsd1* consistently had the most decreased levels in the mutant mESCs compared with WT mESCs (Fig 3B and C, and Appendix Fig S4), arguing that *Lsd1* mRNA may be a functional target of the R783H Trim71 mutant. *Lsd1* (*Kdml1*) is a conserved lysine-specific histone demethylase that is critical for both pluripotency and neural lineage commitment (Whyte et al, 2012; Han et al, 2014). The CLIP-seq data indicated that there is a R783H mutant Trim71-specific binding peak in the 3'UTR of *Lsd1* mRNA, and this peak's signal is significantly higher than that from the size-matched input control (Van Nostrand et al, 2016; Fig 2G), indicating that in mESCs, the mutant Trim71, but not the WT Trim71,

**Figure 2. Transcriptome-wide identification of the target mRNAs of the Trim71 mutant R783H in mESCs.**

- A work flow of the CLIP-seq analysis.
- Distribution of the WT Trim71 and the R783H Trim71 mutant binding regions in the mouse genome. In each CLIP-seq, there are two biological replicates. The binding regions present in both of the biological replicates are used for the analysis.
- Comparison of RNA secondary structures over-represented in the Trim71 mutant R783H and Trim71. "H," "S," and "I" indicates a nucleotide in a hairpin loop region, a stack region, and an internal loop region, respectively.
- Venn diagram showing the genes with binding sites from the WT Trim71 and the Trim71 mutant R783H.
- CLIP-qRT-PCR for the identified target mRNAs of the Trim71 mutant R783H. The results represent the means ( $\pm$ SD) of three independent experiments.
- Gene ontology analysis of the mRNAs with 3'UTR binding sites from the WT Trim71 and the R783H Trim71 mutant.
- UCSC genome browser snapshot for the CLIP-seq data from Trim71 and the Trim71 mutant R783H in the *Lsd1* locus. The red box indicates the binding region of the Trim71 mutant R783H. The inputs are from the size-matched input samples in the CLIP-seq analysis.

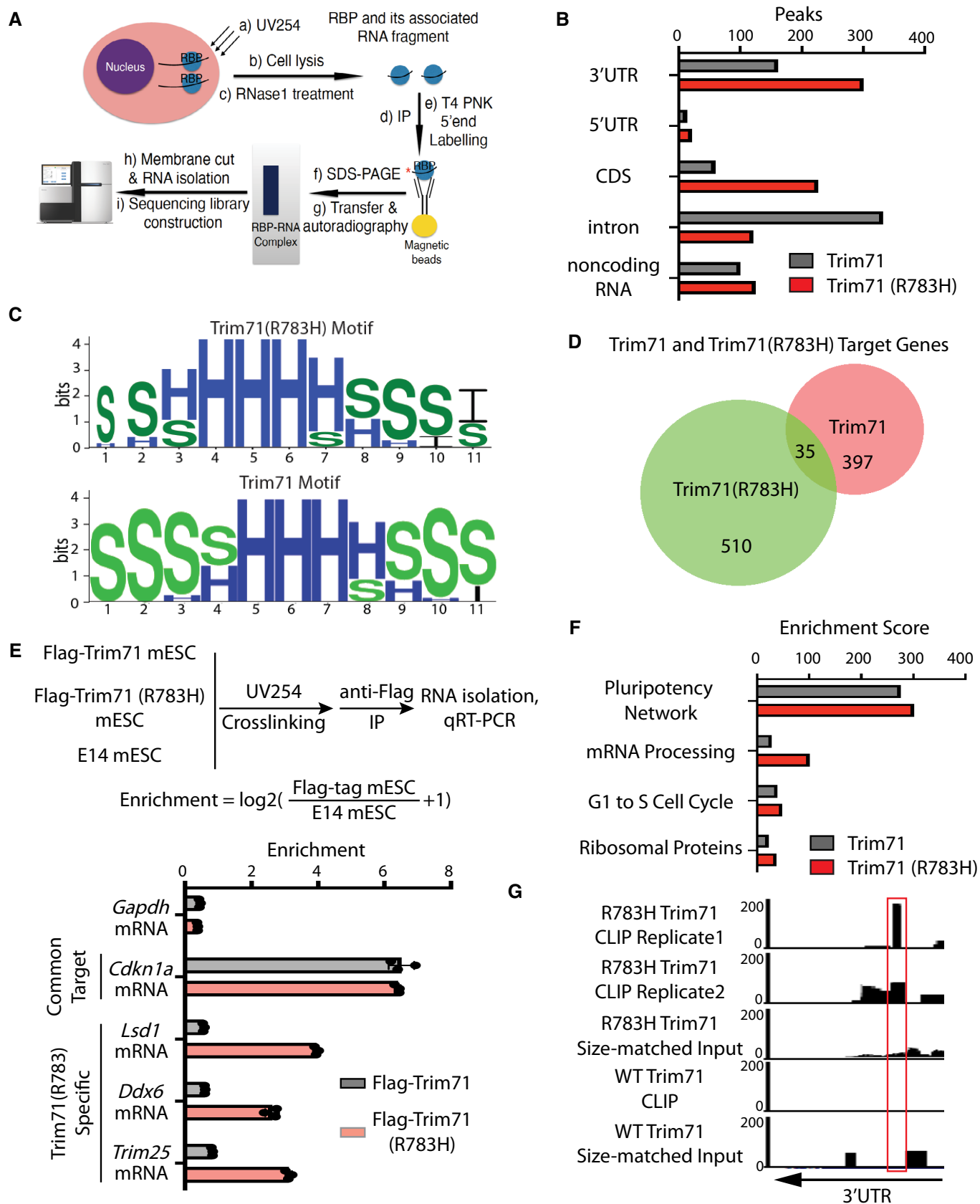
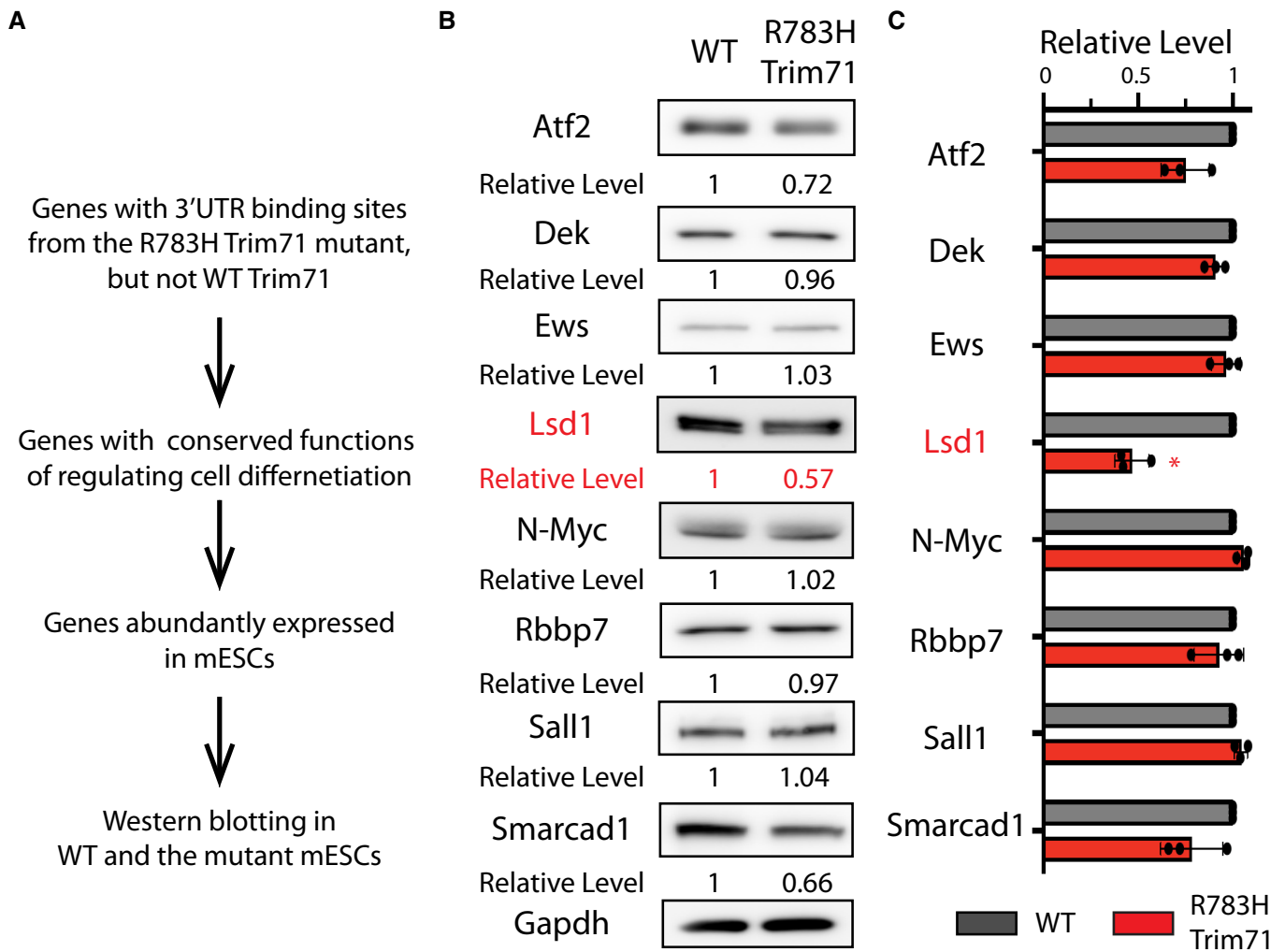


Figure 2.





**Figure 3. Identification of potential functional targets of the R783H Trim71.**

A Outline of strategies to identify potential functional targets of the R783H Trim71.

B A representative set of Western blots in the WT and the R783H Trim71 mESCs.

C Quantification of the target proteins in the WT and the R783H Trim71 mESCs.

Data information: The results represent the means ( $\pm$ SD) of three independent experiments. One-Way ANOVA was used to determine the significance of the difference,

\* $P < 0.05$ . The Western blots listed in (B), is the Biological Replicate one in Appendix Fig S4.

Source data are available online for this figure.

specifically interacts with this region of *Lsd1* mRNA. In the subsequent experiments, we focused on the interaction between *Lsd1* (*Kdm1a*) mRNA and the mutant Trim71.

### R783H Trim71 represses *Lsd1* mRNA translation

Multiple lines of evidence indicated that the R783H Trim71 mutant represses *Lsd1* mRNA translation in mESCs. First, *Lsd1* protein decreased ~2 fold with no significant changes in the level of *Lsd1* mRNA in mutant mESCs compared with WT mESCs (Fig 4A and B). Second, polysome analysis, which examines mRNA and ribosome association, revealed that *Lsd1* mRNA, but not a control mRNA, is translationally repressed in mutant mESCs compared to WT mESCs (Fig 4C and D). Third, when ectopically expressed in the WT

mESCs, the R783H Trim71 mutant, but not WT Trim71, decreased *Lsd1* protein levels without altering its mRNA levels (Fig 4E and F), and specifically reduced the association of *Lsd1* mRNA with polyribosomes (Fig 4G and H). Altogether, these results indicated that the translation of *Lsd1* mRNA was specifically repressed by the R783H Trim71 mutant.

This repression is dependent on the binding of the mutant Trim71 to the 3'UTR of *Lsd1* mRNA. Because in the *Lsd1* CLIPa mESCs, where the interaction between *Lsd1* mRNA 3'UTR and the mutant Trim71 was abolished (see below), the mutant Trim71 failed to decrease both *Lsd1* protein level and *Lsd1* mRNA's association with polyribosomes in mESCs (Appendix Fig S5A–C).

The sequence of the *Lsd1* mRNA 3'UTR is not conserved between mouse and human. However, similar stem-loop structures

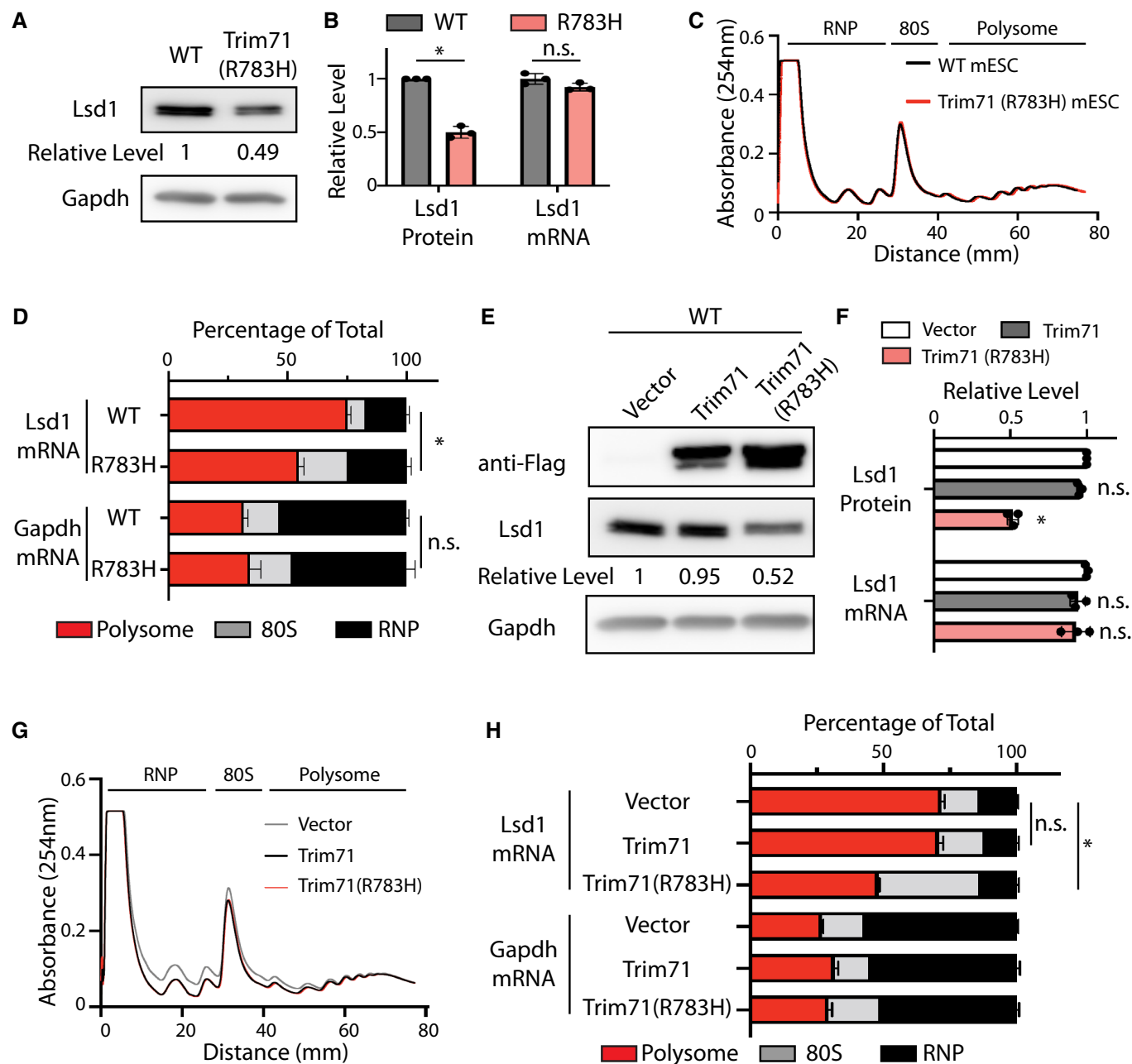


**Figure 4. Trim71 mutant R783H represses *Lsd1* mRNA translation in mESCs.**

- A Western blotting in the WT and the Trim71 (R783H) mESCs.
- B Quantification of Lsd1 protein and mRNA levels. Gapdh and 18S rRNA were used for normalization in protein and mRNA quantifications, respectively.
- C Polysome analysis in the WT and the Trim71 (R783H) mESCs.
- D Quantification of the indicated mRNA distribution in the RNP, 80S, and polysome fractions from the WT and the Trim71 (R783H) mESCs.
- E Western blotting in the WT mESCs expressing an empty vector, Flag-Trim71, Flag-Trim71 (R783H).
- F Quantification of Lsd1 protein and mRNA in the WT mESCs expressing an empty vector, Flag-Trim71, Flag-Trim71 (R783H).
- G Polysome analysis in the WT mESCs expressing an empty vector, Flag-Trim71, Flag-Trim71 (R783H).
- H Quantification of the indicated mRNA distribution in the RNP, 80S, and polysome fractions from the WT mESCs expressing an empty vector, Flag-Trim71, Flag-Trim71 (R783H).

Data information: The quantification results in (B, D, F, and H), represent the means (±SD) of three independent experiments. \* $P < 0.05$ ; and n.s., not significant ( $P > 0.05$ ) by One-Way ANOVA.

Source data are available online for this figure.

recognized by the mutant Trim71 (Fig 2C) are predicted *in silico* to be present in the 3'UTR of human *LSD1* mRNA, suggesting that the corresponding mutant human TRIM71 may also be able to repress *LSD1*. To test this, we expressed WT and the corresponding R796H mutant TRIM71 in NCCIT cells, which are human embryonal carcinoma cells. The human mutant TRIM71, but not WT TRIM71, reduced LSD1 protein levels without significantly changing *LSD1* mRNA levels (Appendix Fig S6), similar to the results in mESCs (Fig 4E and F), indicating the ability of the CH-causing Trim71 mutation to repress Lsd1 expression is conserved between mouse and human.

To determine how the R783H Trim71 represses mRNA translation, we used the tethering assays. We observed that similar to the WT Trim71, the R783H Trim71 repressed luciferase production without decreasing luciferase mRNA levels when tethered to the 3'UTR of a luciferase reporter mRNA via the specific interaction between the bacteriophage  $\lambda$ N polypeptide and the BoxB RNA motif (Fig EV4A and B). Additionally, when tethered to the IRES (internal ribosome entry site)-containing bicistronic dual-luciferase reporters (Fig EV4C), the R783H Trim71 represses the translation driven by both HCV-IRES and CrPV-IRES (Fig EV4D and E). Since HCV-IRES requires all the initiation factors except eIF4G and eIF4E, CrPV-IRES only requires 40S ribosomal subunit for initiating translation (Fraser & Doudna, 2007), these results argued that the R783H Trim71 represses translation at an event at or after the 60S ribosomal subunit joining step. Furthermore, when tethered to a luciferase reporter mRNA that is devoid of both a poly(A) tail and the poly(A) tail binding protein Pabpc1 (Zhang et al, 2017), the R783H Trim71 can still repress the translation of this poly(A) minus mRNA (Fig EV4F–H). Poly(A) tail and Pabpc1 facilitate several steps in mRNA translation, such as 40S ribosomal subunit recruitment and the 60S ribosomal subunit joining (Kahvejian et al, 2005). The results from this poly(A) minus reporter, together with the findings from the IRES-containing bicistronic reporters, argues that the R783H Trim71 modulates mRNA translation at a postinitiation step(s). Moreover, in all these tethering assays, the R783H Trim71 functioned similar to the WT Trim71 (Fig EV4), suggesting that these two proteins repress mRNA translation via the same mechanisms. This is consistent with the observation that the R783H mutation is within the RNA-binding domain but not in the domains involved in translational repression in Trim71 (Loedige et al, 2013).

### Specific inhibition of *Lsd1* repression alleviates stem cell and neural differentiation defects

To evaluate the functional relevance of the mutant-Trim71-mediated translational repression of *Lsd1* mRNA to the differentiation defects of the mutant mESCs, we generated bi-allelic deletion of the mutant Trim71-binding region (~60 bp), defined from the CLIP-seq (Fig 2G), in the 3'UTR of *Lsd1* using genome editing (Fig 5A). We named this deletion as Lsd1 CLIP $\Delta$ . CLIP-qRT-PCR indicated that in the Lsd1 CLIP $\Delta$  mESCs the interaction between *Lsd1* mRNA and the mutant Trim71 was specifically disrupted. Because the mutant Trim71 did not bind *Lsd1* mRNA, but still specifically interacted with other target mRNAs, such as *Cdkn1a* mRNA and *Ddx6* mRNAs (Fig 5B). Thus, the Lsd1 CLIP $\Delta$  enabled us to specifically examine the functional significance of the mutant-Trim71:*Lsd1*-mRNA interaction at both molecular and cell function levels.

At the molecular level, the Lsd1 CLIP $\Delta$  increased Lsd1 protein in the mutant Trim71 mESCs to a level similar to that in WT mESCs (Fig 5C and D). *Lsd1* mRNA, however, was not significantly increased (Fig 5D), further confirming the translational repression mediated by the R783H Trim71 mutant. Notably, unlike the observations in R783H Trim71 mutant mESCs, the Lsd1 CLIP $\Delta$  did not increase Lsd1 protein levels in WT mESCs (Fig 5C), indicating that the Lsd1 CLIP $\Delta$  sequence in the 3'UTR of *Lsd1* mRNA does not regulate Lsd1 production *in cis*, but controls *Lsd1* mRNA translation through interacting with the mutant Trim71. Moreover, in the Lsd1 CLIP $\Delta$  background, the R783H mutation did not alter the polysome association of *Lsd1* mRNA (Appendix Fig S7), which is different from the results in the WT background (Fig 4C and D), indicating that the translation repression requires the binding of the R783H Trim71 mutant to *Lsd1* mRNA. These findings, combined with the R783H Trim71 mutant CLIP-seq results, revealed that the CH-causing mutation significantly alters, but does not abolish, RNA target recognition by Trim71.

At the cell function level, the Lsd1 CLIP $\Delta$  abolished the stem cell differentiation defects of the R783H Trim71 mutant mESCs, as indicated by both the exit pluripotency assay (Fig 5E) and the expression level of pluripotency markers during EB formation (Fig 5F). Moreover, during neural differentiation, the Lsd1 CLIP $\Delta$  alleviated the accelerated neural differentiation in the mutant Trim71 mESCs. This was manifested as a decrease in Pax6 when the Lsd1 CLIP $\Delta$  was introduced in the mutant mESCs (Fig 5G). However, no

#### Figure 5. Specific inhibition of the interaction between the Trim71 mutant R783H and *Lsd1* mRNA alleviates the stem cell and neural differentiation defects in the Trim71 (R783H) mESCs.

- A Deletion of the Trim71 mutant R783H binding site in *Lsd1* mRNA's 3'UTR.
- B CLIP-RIP followed by qRT-PCR to examine mRNAs associated with the Trim71 and the Trim71 mutant R783H in the WT, Trim71 (R783H), CLIP $\Delta$ , and Trim71 (R783H)/CLIP $\Delta$  mESCs. The mRNA signals from the E14 mESCs were set as 1 for relative comparison.
- C Western blotting in the WT, Trim71 (R783H), CLIP $\Delta$ , and Trim71 (R783H)/CLIP $\Delta$  mESCs.
- D Quantification of Lsd1 protein and mRNA in the WT, Trim71 (R783H), CLIP $\Delta$ , and Trim71 (R783H)/CLIP $\Delta$  mESCs. Beta-Tubulin and 18S rRNA were used for normalization in the protein and mRNA quantification, respectively.
- E Exit pluripotency assay for mESCs.
- F Representative Western blotting and quantification of pluripotency factors during EB formation.
- G Representative Western blotting and quantification of neural lineage markers during mESCs neural differentiation.

Data information: The results from (B, D, F, and G), represent the means ( $\pm$ SD) of three independent experiments. In (E), the colony morphology and AP intensity were evaluated through microscopy. One hundred to 200 colonies were examined each time to determine the percentage of undifferentiated colonies. \* $P < 0.05$ ; and n.s., not significant ( $P > 0.05$ ) by One-Way ANOVA.

Source data are available online for this figure.



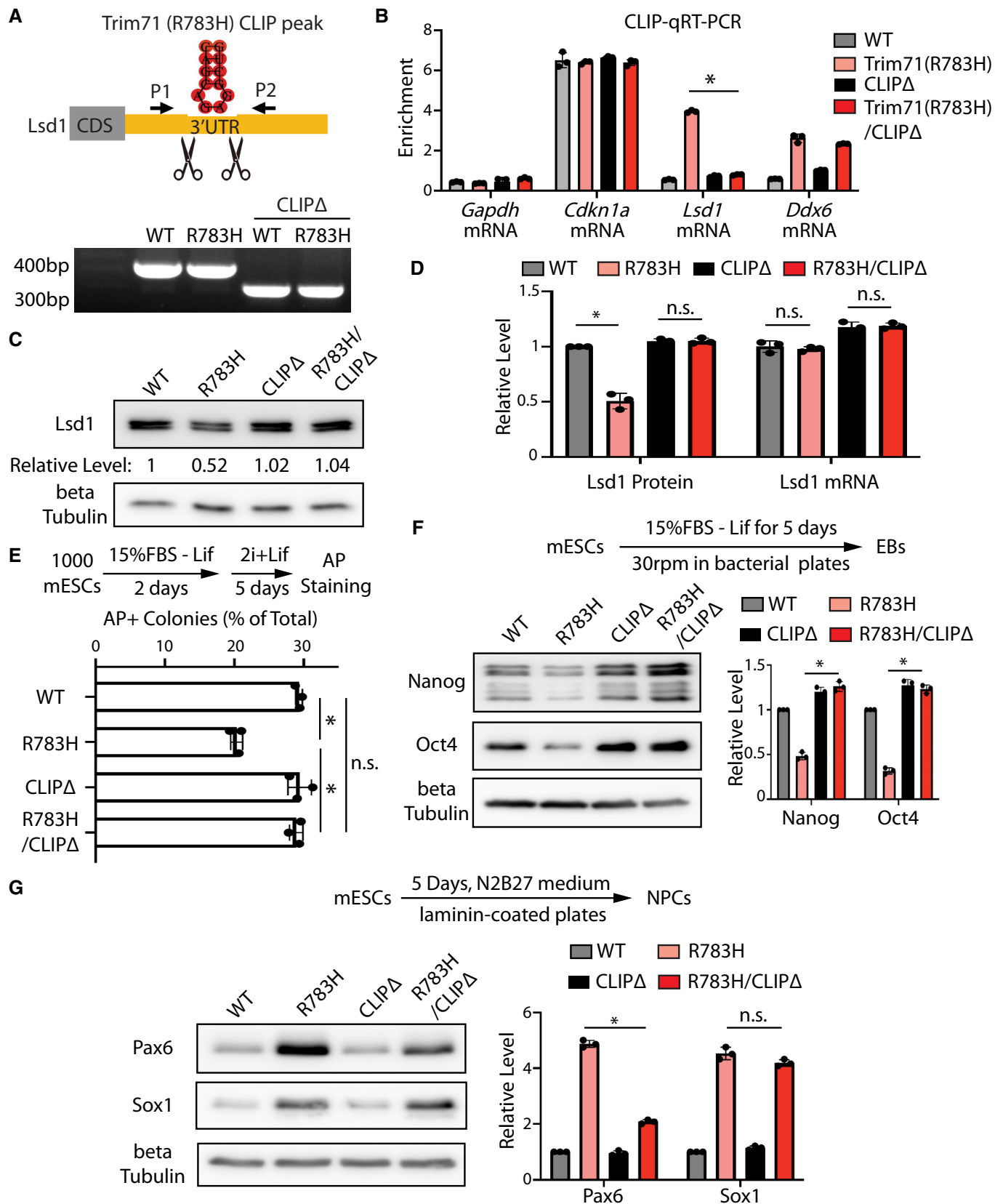


Figure 5.

significant changes in Sox1 were observed (Fig 5G). This is possibly due to additional functional targets of the R783H Trim71 mutant during neural differentiation. Nevertheless, these results collectively indicate that repression of *Lsd1* mRNA translation by the R783H Trim71 mutant is required for the stem cell and neural differentiation defects in the R783H Trim71 mESCs.

### Increasing Lsd1 alleviates the stem cell and neural differentiation defects

To evaluate the functional significance of Lsd1 in the differentiation defects seen in the CH-causing R783H mutation, we asked whether increasing Lsd1 protein levels could mitigate the phenotypes of the mutant mESCs. For this purpose, we generated stable mESC lines in which the expression of an Lsd1-GFP fusion protein can be induced by doxycycline (dox) in a dosage-dependent manner (Fig 6A). The GFP fusion enabled us to discriminate exogenous Lsd1 from endogenous Lsd1. Modulation of dox levels revealed that a ~25% increase in Lsd1 protein levels over endogenous levels alleviated the differentiation defects seen in the mutant mESCs, as revealed by both the exit pluripotency assay (Fig 6B) and the expression level of

pluripotency markers during differentiation (Fig 6C). This alleviation is specific to the mutant mESCs, as expression of exogenous Lsd1 at a similarly increased level did not cause phenotypical changes in WT mESCs (Fig 6A–C). Moreover, this alleviation requires the demethylase activity of Lsd1, because expressing a demethylase catalytic mutant of Lsd1 (Chen *et al*, 2006; Kim *et al*, 2020) failed to mitigate the differentiation defects of the mutant mESCs (Fig EV5A–C). During neural differentiation, similar to the result from the Lsd1 CLIPA approach (Fig 5G), although not decreasing Sox1 to the normal level, the slightly (~25%) increased Lsd1 reduced the overexpressed Pax6 in the mutant mESCs (Fig 6D), indicating that increasing Lsd1 mitigates the neural differentiation defects in the mESCs with the CH-causing mutation. Thus, decreased Lsd1 protein levels in R783H Trim71 mutant mESCs plays a critical role in the observed stem cell and neural differentiation defects.

### Lsd1 plays an important role in the differentiation defects in mESCs with mono-allelic R783H mutation on Trim71

A caveat of the above results is that although the bi-allelic R783H Trim71 mutation in mESCs provides critical functional and

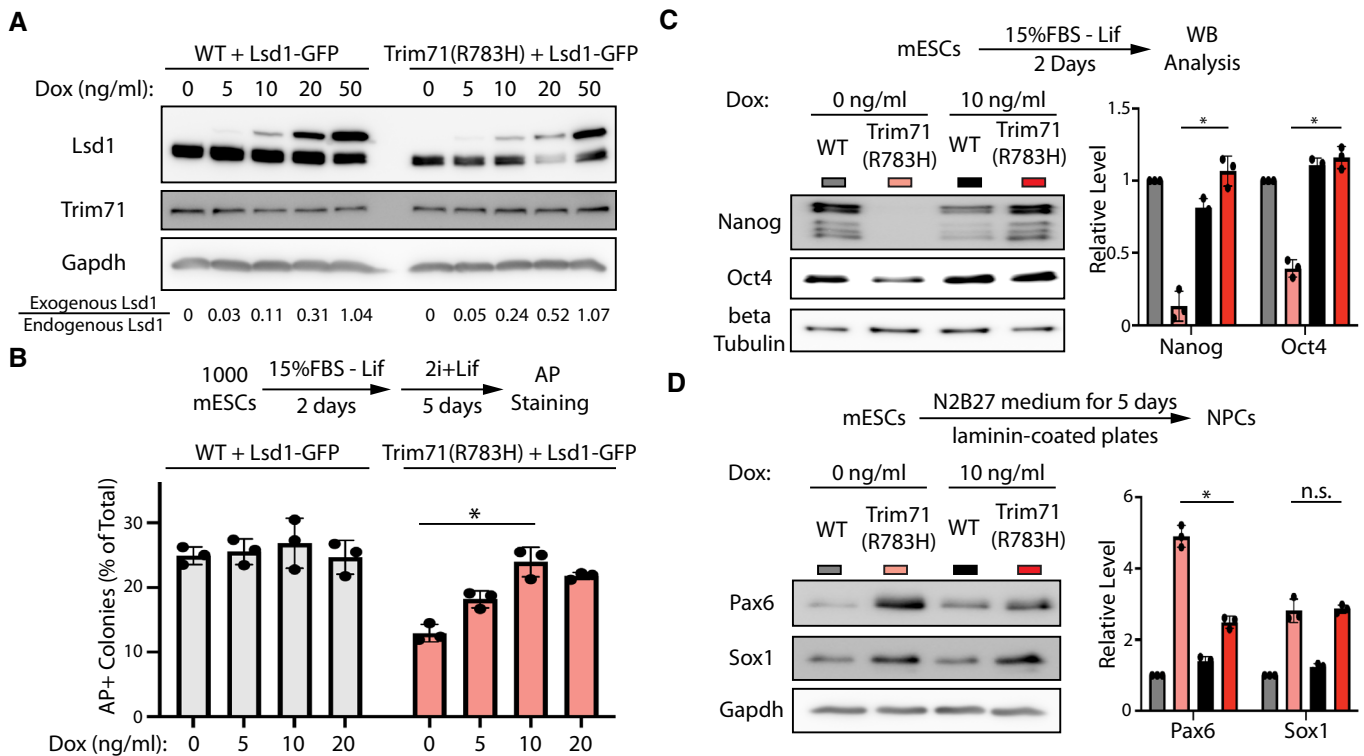


**Figure 6. Slight increase in Lsd1 alleviates the stem cell and neural differentiation defects in the Trim71(R783H) mESCs.**

- A Western blotting in the WT and the Trim71 (R783H) mESCs with dox-inducible expression of Lsd1-GFP.  
 B Exit pluripotency assay for mESCs.  
 C Representative Western blotting and quantification of pluripotency factors during the monolayer differentiation of mESCs.  
 D Representative Western blotting and quantification of neural lineage markers during mESCs neural differentiation.

Data information: In (B), the colony morphology and AP intensity were evaluated through microscopy. One hundred to 200 colonies were examined each time to determine the percentage of undifferentiated colonies. The quantification results from (B, C, and D), represent the means ( $\pm$ SD) of three independent experiments.

\* $P < 0.05$ ; and n.s., not significant ( $P > 0.05$ ) by One-Way ANOVA.

Source data are available online for this figure.

mechanistic insights into the mutant Trim71, it is the mono-allelic R783H mutation that causes CH. To evaluate whether the mechanistic insights we obtained using bi-allelic R783H mESCs are relevant to the pathogenesis of the disease, we examined mESCs with a mono-allelic R783H mutation in Trim71 (R783H/+; Fig EV1B), which mimics the genetic setting of CH. The R783H/+ mESCs displayed similar stem cell and neural differentiation defects as the bi-allelic R783H mESCs, as indicated by decreased Lsd1 protein levels

(Fig 7A), rapid exit from pluripotency (Fig 7B and C), and accelerated neural differentiation (Fig 7D).

To determine whether increasing Lsd1 level reduce these stem cell and neural differentiation defects in mESCs with the mono-allelic mutation, we used dox-inducible expression of Lsd1-GFP in the R783H/+ mESCs (Fig 7E). Expression of exogenous Lsd1-GFP in R783H/+ mESCs alleviated the defects in stem cell differentiation (Fig 7F and G) and neural lineage commitment (Fig 7H). Thus, in

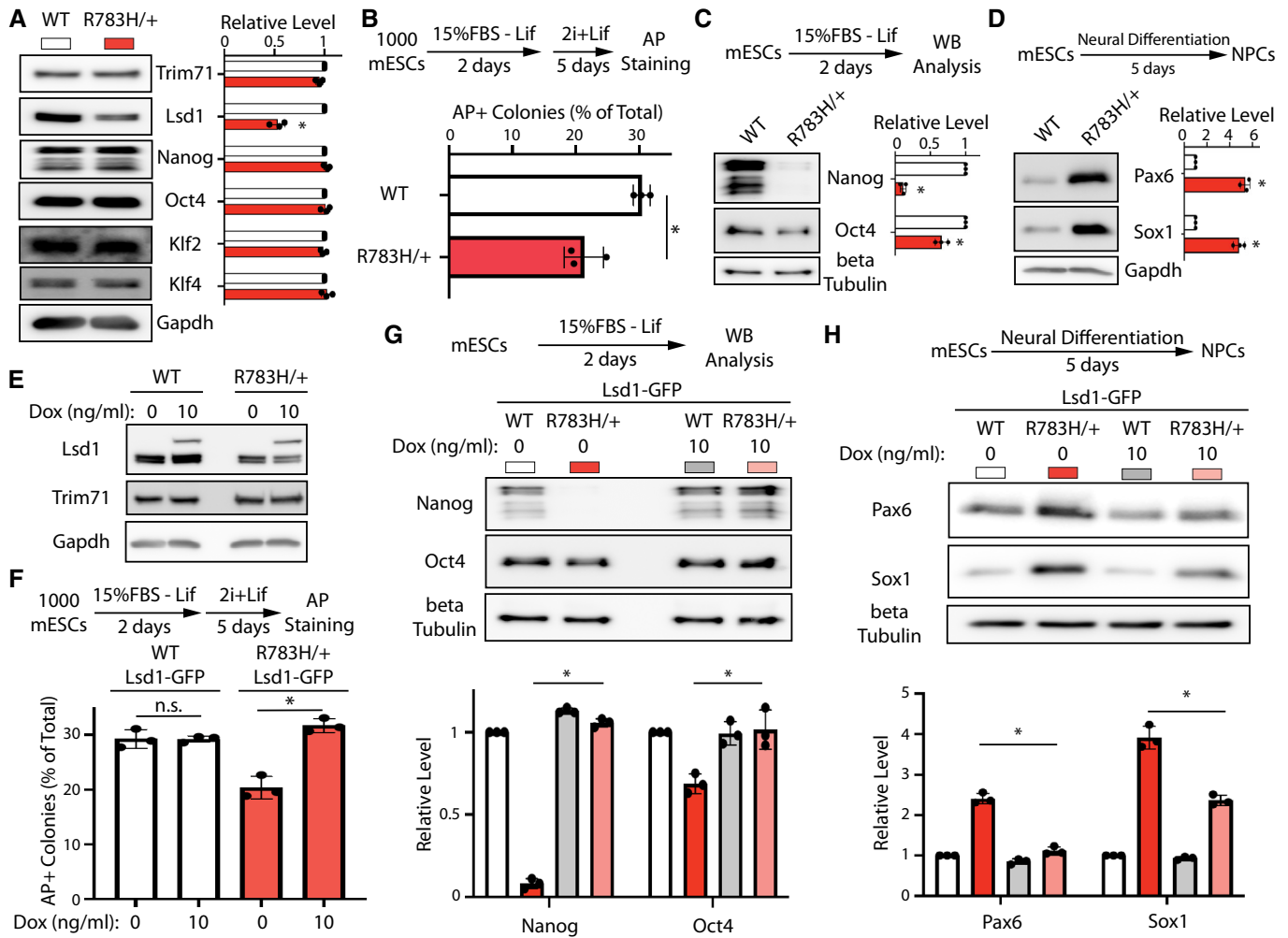


**Figure 7. Mono-allelic R783H mutation on Trim71 results in stem cell and neural differentiation defects in a Lsd1 dependent manner.**

- A Representative Western blotting and quantification in the WT and the R783H/+ mESCs.
- B Exit pluripotency assay for the WT and the R783H/+ mESCs.
- C Representative Western blotting and quantification of pluripotency factors in differentiating mESCs.
- D Representative Western blotting and quantification of neural lineage markers during mESCs neural differentiation.
- E Western blotting in the WT and the R783H/+ mESCs with dox-inducible expression of Lsd1-GFP.
- F Exit pluripotency assay for the WT and the R783H/+ mESCs with dox-inducible expression of Lsd1-GFP.
- G Representative Western blotting and quantification of pluripotency factors during the differentiation of the WT and the R783H/+ mESCs with dox-inducible expression of Lsd1-GFP.
- H Representative Western blotting and quantification of neural lineage markers during the neural differentiation of the WT and the R783H/+ mESCs with dox-inducible expression of Lsd1-GFP.

Data information: In (B and F), the colony morphology and AP intensity were evaluated through microscopy. In each biological replicate, 100–200 colonies were examined each time to determine the percentage of undifferentiated colonies. The quantification results from (A, B, C, D, F, G, and H) represent the means (±SD) of three independent experiments. \**P* < 0.05; and n.s., not significant (*P* > 0.05) by One-Way ANOVA. Source data are available online for this figure.

the CH-mimic setting, a slight increase in Lsd1 protein levels can also mitigate the stem cell differentiation defects caused by the mutant Trim71.

## Discussion

Here, we show that, in mouse embryonic stem cells, the CH-causing R783H Trim71 gain-of-function mutation resulted in defects in stem cell differentiation and neural lineage commitment, both in the mono-allelic condition, as found in human patients, and the bi-allelic condition. Mechanistically, the R783H Trim71 mutation significantly changes the mRNA substrates to which Trim71 binds and potentially regulates in mESCs. Among the newly acquired mRNA substrates, we determined that the mutant Trim71 represses *Lsd1* mRNA translation. Specific inhibition of *Lsd1* translational repression or mild overexpression of Lsd1, both of which increase Lsd1 protein levels, alleviate the differentiation defects in mESCs expressing the CH-causing R783H Trim71 mutation. These results provide mechanistic insights into the pathogenesis of CH mediated by the R783H mutation in Trim71 and argue that Lsd1 can be a potential therapeutic target for CH.

### Trim71 target recognition

Previous studies show that the CH-causing mutations in Trim71 result in a loss of interactions with many Trim71's target mRNAs (Welte *et al*, 2019; Duy *et al*, 2022), and the Trim71 mutants may associate with new mRNAs (Foster *et al*, 2020). Although the difference among these studies and ours can be explained by different cellular context, our findings are in agreement with the observation that the CH-causing mutations lead to the loss of interactions with many WT Trim71 target mRNAs. However, in addition to the loss, we found that the R783H mutation in Trim71 also enable Trim71 to bind a new set of target mRNAs (Fig 2D). Thus, this CH-causing mutation does not abolish, but significantly changes Trim71's binding specificity for target mRNAs (Fig 2D). Given that both WT Trim71 and R783H Trim71 interact with mRNAs that share similar predicted secondary structure motifs (Fig 2C), the molecular basis for their differing target specificities is unclear. Trim71, a highly conserved RBP, binds target RNAs through its NHL domain. Structural and *in vitro* binding studies indicate that the binding specificity of the NHL domain is determined by the shape of an RNA stem-loop structure and not by the primary sequence motifs (Kumari *et al*, 2018). Based on a crystal structure of the NHL domain from *Drosophila melanogaster* Brat (Loedige *et al*, 2015), a close homolog of Trim71, the R796H mutation (R783H in mouse) is predicted to alter the interaction between Trim71 and RNA's phosphate backbone (Furey *et al*, 2018). We speculate that the point mutation impacts RNA structural shape recognition, altering target mRNA binding. Consistent with this notion, comparison of the CLIP-seq datasets revealed that the major difference between WT and mutant Trim71 is a decreased stringency in the stem region of the predicted stem-loop/hairpin structure enriched in the mutant-Trim71-binding regions (Fig 2C).

However, the enriched structural motifs identified using CLIP-seq are likely necessary, but not sufficient, for the binding. Because similar structural motifs can be predicted *in silico* outside Trim71-binding regions defined by CLIP-seq in target mRNAs and in non-target

mRNAs. This implies that besides the structural motifs, additional features are involved in Trim71's target recognition. Furthermore, it is unclear whether and when the *in silico* predicted secondary structures are formed *in vivo*. Unlike *in vitro* folding, formation of RNA structures *in vivo* is constrained by contexts (e.g., RBPs in the neighboring region). Thus, future structural studies on Trim71 combined with *in vivo* probing of RNA structures will reveal how Trim71 specifically recognizes its targets and how mutations alter this process.

### Characterization of functional RBP:mRNA Interactions

CLIP is widely used in identifying *in vivo* RBP:RNA interactions (Lee & Ule, 2018; Hafner *et al*, 2021); and, when combined with high-throughput sequencing, this method has revealed transcriptome-wide binding sites and the corresponding target genes for many RBPs (Van Nostrand *et al*, 2020). However, opportunistic or nonproductive interactions can complicate identifying functional targets. While loss-of-function (knockout/knockdown) and gain-of-function (overexpression) approaches can determine RBPs' functions, these methods, however, provide limited insights into the significance of specific RBP:RNA interactions. Because an RBP usually binds and potentially regulates numerous RNAs, and knockout or overexpression of an RBP can lead to alteration in many RBP:RNA interactions, making assigning any phenotypic changes to specific RBP:RNA interactions challenging.

Here, we specifically disrupted the interaction between the R783H Trim71 mutant and *Lsd1* mRNA, by deleting the 3'UTR binding site identified using CLIP-seq (Fig 5A). This approach does not abolish the interactions between the mutant Trim71 and its other target mRNAs (Fig 5B), thereby we could specifically evaluate the role of this interaction plays in the R783H Trim71 mediated mESC differentiation defects. We believe similar approaches will reveal many more functional RBP:mRNA interactions in normal and pathological processes.

### Lsd1 and neural differentiation

Lsd1 is a conserved histone lysine-specific demethylase with critical functions in stem cell biology (Adamo *et al*, 2011; Whyte *et al*, 2012). Besides histone, Lsd1 can also modulate the methylation status of other proteins (e.g., p53; Perillo *et al*, 2020). Previous studies indicated that the elimination of Lsd1 through proteasome-mediated degradation promotes mESC differentiation toward neural lineage (Han *et al*, 2014). Here, we found that the CH-causing Trim71 mutant (R783H) binds to *Lsd1* mRNA and repress its translation, leading to accelerated stem cell differentiation and premature neural lineage commitment.

When regulating histones in chromatin, Lsd1 can both activate and repress gene expression through association with different histone modification complexes (Kozub *et al*, 2017). We found that the ~50% reduction in Lsd1 protein levels in R783H Trim71 mESCs, mediated by translational repression, results in differentiation defects (Fig 5), while a ~25% increase in Lsd1 protein levels in the same R783H Trim71 mESCs alleviates these defects (Fig 6). These observations argue that genes controlled by weak/dynamic Lsd1 binding may mediate the differentiation defects in the mutant mESCs. Because weak/dynamic interactions are more sensitive to concentration fluctuations than strong/steady interactions. Numerous Lsd1 target genes have been identified using ChIPs (chromatin immunoprecipitations); however, the formaldehyde crosslinking step makes quantitatively

discriminating weak versus strong chromatin:protein interactions challenging. Thus, noncrosslinking approaches, such as CUT&Tag (Kaya-Okur *et al*, 2019), may be more suitable for identifying those weak/dynamic Lsd1 chromatin targets altered in the mutant mESCs. It is also possible that the decreased Lsd1 in the mutant mESCs may change the methylation status, thereby modulating the activity/function, of non-histone proteins. Characterizing such potential functional targets of Lsd1 may reveal novel regulators of neural differentiation.

Finally, it is important to mention that although we identified *Lsd1* mRNA as a critical functional target of the R783H Trim71 mutant, it is likely not the only functional target, because the altered Lsd1 protein levels can only partially explain the neural differentiation defects. The differentiation defects in the R783H

mESCs can be contributed by the newly obtained mRNA targets of the R783H Trim71 mutant, or alternatively, by the loss of the binding to the WT Trim71 target mRNAs. However, since the R783H mutant mESCs displayed different phenotypes from the Trim71 knockout mESCs in terms of proliferation (Fig EV2A and B) and differentiation (Fig 1C–F), it strongly argues that the defects in the R783H mutant mESCs are from the mRNA targets unique to the R783H Trim71. Interestingly, besides *Lsd1* mRNA, several other target mRNAs of R783H Trim71 also encode important regulators of stem cell differentiation, as such *Ddx6* (Di Stefano *et al*, 2019). Future functional characterization of these additional target mRNAs will reveal further insights into the pathogenesis of this CH-causing mutation on Trim71.

## Materials and Methods

### Reagents and Tools table

Reagent/Resource	Reference or Source	Identifier or Catalog Number
<b>Antibodies</b>		
Mouse monoclonal anti-FLAG M2	Sigma-Aldrich	Cat# F1804
Rabbit monoclonal anti-Nanog (D2A3)	Cell Signaling Technology	Cat# 8822
Mouse monoclonal anti-Oct-4	BD Transduction Laboratories™	Cat# 611202
Rabbit monoclonal anti-Sox2 (D9B8N)	Cell Signaling Technology	Cat# 23064
Rabbit monoclonal anti-beta-Tubulin	Selleckchem	Cat# A5032
Rabbit anti-Pax6	Antibodies-online Inc.	Cat#ABIN3043379
Rabbit anti-Sox1	Cell Signaling Technology	Cat#4194
Mouse anti-LSD1	Cell Signaling Technology	Cat#4064
Mouse monoclonal anti-GAPDH (6C5)	Santa Cruz Biotechnology	Cat# sc-32233
Goat Anti-Rabbit IgG (H L)-HRP Conjugate	Bio-Rad	Cat# 170-6515
Goat Anti-Mouse IgG (H L)-HRP Conjugate	Bio-Rad	Cat# 170-6516
Rabbit anti DEK (E1L3V)	Cell Signaling Technology	Cat#13962
Rabbit anti N-Myc (D1V2A)	Cell Signaling Technology	Cat#84406
Mouse anti-SALL1	Abcam	Cat#ab41974
Mouse anti-SMARCAD1	Abcam	Cat#ab67548
Rabbit anti-RBAP46 (V415)	Cell Signaling Technology	Cat#6882
Rabbit anti-EWS	Cell Signaling Technology	Cat#11910
Rabbit anti-ATF2 (D4L2X)XP	Cell Signaling Technology	Cat#35031
<b>Oligonucleotides</b>		
qPCR primers for LSD1: Forward: GTGGTGTATGCTTTGACCGT Reverse: GCTGCCAAAATCCCTTTGAGA	This study	oWH5081 oWH5082
qPCR primers for Cdkn1a: Forward: CCTGGTGATGTCCGACCTG Reverse: CCATGAGCGCATCGCAATC	Liu <i>et al</i> (2021a, 2021b)	oWH1432 oWH1433
qPCR primers for Ddx6: Forward: CCAGCACAAATCAATAATGGCAC Reverse: GGAGGTCACATCCGAAGTTTTC	This study	oWH5399 oWH5400
qPCR primers for Gapdh: Forward: GCAAAGTGGAGATTGTGCCAT Reverse: CCTTGACTGTGCCGTTGAATTT	Liu <i>et al</i> (2021a, 2021b)	oWH170 oWH171



**Reagents and Tools table** (continued)

sgRNA for introducing R783H mutation on mouse Trim71: TGGGCAGTTCCTGCGACCAC	This study	oWH4229
Donor oligo for introducing R783H mutation on mouse Trim71: CACCTGATTGCCAATCTGCCCGCTTCTGGGTTCCGAGGGCTC cGGAATGGGCAGTTCCTGCACCCACAGGGTGTGGCTGTGGAC CAGGAAGGGAGAATCATCGTAGCC	This study	oWH4189
Genotyping primers for mouse Trim71R783H: Forward: AGGGCAAGATCCTCGTTTCA Reverse: CACGACGATCAATCCATCCG	This study	oWH4977 oWH4978
Dual sgRNAs for deleting the Trim71-R783H binding region in the 3'UTR of mouse LSD1 mRNA: sgRNA1: agctgtacttccaaatcaat sgRNA2: agtagctgatgacatggagt	This study	oWH5077 oWH5078
Genotyping primers for deleting the Trim71-R783H binding region in the 3'UTR of mouse LSD1 mRNA: Forward: gaggttatctcacaccactgtctctc Reverse: ctgcacagcagctcccaagtatg	This study	oWH5079 oWH5080
qPCR primers for mouse Trim25: Forward: ATGGCTCAGGTAACAAGGGAG Reverse: GGGAGCAACAGGGGTTTCTT	This study	oWH5401 oWH5402
qPCR primers for human Lsd1: Forward: TGACCGGATGACTTCTCAAGA Reverse: GTTGAGAGTAGCCTCAAATGTC	This study	oWH5615 oWH5616
qPCR primers for human 18S: Forward: cgcagctaggaataatggaatagg Reverse: catggcctcagttcccga	This study	oWH703 oWH704
<b>Plasmids</b>		
sgRNA and Cas9 expressing vector (pX458) pWH464	Addgene	Cat# 48138
Super PiggyBac Transposase expressing vector (pWH252)	System Biosciences	Cat# PB210PA-1
Inducible GFP expressing vector	Liu et al (2021a, 2021b)	pWH1055
Inducible mouse FLAG-Trim71 expressing vector	Liu et al (2021a, 2021b)	pWH826
Inducible mouse FLAG-Trim71R783H expressing vector	This study	pWH1101
Inducible mouse LSD1-GFP expressing vector	This study	pWH1223
Inducible human 3xHA-Trim71 expressing vector	This study	pWH983
Inducible human 3xHA-Trim1R796H expressing vector	This study	pWH1158

**Methods and Protocol****Cell culture**

All the mouse ESCs used in this study are derived from ES-E14TG2a (ATCC CRL-1821), which was authenticated by STR profiling and tested negative for mycoplasma. mESCs were cultured on 0.5% gelatin-coated tissue cultured plates, in either 15% FBS + Lif medium or 2i + Lif medium (Mulas et al, 2019). Human cell line NCCIT (ATCC, CRL-2073) was maintained in RPMI-1640 medium supplemented with 10% FBS. All cells were incubated at 37°C with 5% CO<sub>2</sub>.

**CRISPR/Cas9-mediated genome editing in mESCs**

To generate the FLAG-Trim71R783H mESCs and FLAG-Trim71R783H<sup>+/-</sup> mESCs, FLAG-Trim71 mESCs were co-transfected with 2 µg of pWH464 (pSpCas9(BB) – 2A-GFP (pX458)) carrying the targeting sgRNA (oWH4229) and 1 µg of donor oligo (oWH4189) using Fugene6. To generate Lsd1 CLIPa cells, 2 µg of pWH464 expressing a pair of sgRNAs targeting the indicated region

was transfected into the mESCs. Transfected cells were single-cell sorted to 96-well plates. Colonies were then picked and expanded for validation by genotyping PCR followed by sequencing and Western blot analysis.

**Generation of stable cell lines**

Stable cell lines expressing doxycycline-inducible mouse FLAG-Trim71, mouse FLAG-Trim71R783H, mouse LSD1-GFP, human 3xHA-Trim71, or human 3xHA-Trim71R796H were generated using a PiggyBac transposon-based expression system. Briefly, cells were co-transfected with indicated plasmids and PiggyBac transposase (pWH252). After 48 h, cells were selected with 1 µg/ml puromycin for 4 days.

**RNA extraction and RT-qPCR**

RNA was extracted from cells using RNA reagent and treated with DNase1 to remove contaminating DNA. cDNA was synthesized using random hexamers and Superscript2 reverse transcriptase (Invitrogen) according to the manufacturer's instructions. qPCR was

performed in triplicate for each sample using the SsoAdvanced Universal SYBR Green Supermix (Bio-Rad) and a CFX96™ real-time PCR detection system (Bio-Rad).

#### Western blotting

Proteins were harvested in RIPA buffer (10 mM Tris-HCl pH 8.0, 140 mM NaCl, 1 mM EDTA, 1% Triton X-100, 0.5 mM EGTA, 0.1% SDS, 0.1% sodium deoxycholate, and protease inhibitor cocktail) and quantified with BCA assay kit. Protein samples were resolved by SDS-PAGE and then transferred to PVDF membranes. Western blotting was performed using a BlotCycler (Precision Biosystems) with the indicated antibodies. Signals were developed with the Western ECL substrate (Bio-Rad) and detected with an ImageQuant LAS 500 instrument (GE Healthcare).

#### Colony formation assay and exit from pluripotency assay

For colony formation assay, 500 cells per well were plated on a 12-well plate in 15% FBS + Lif medium for 6 days. For exit from pluripotency assay, 1,000 cells per well were plated on six-well plates in differentiation media (15% FBS – Lif) for 2 days, then cultured in 2i + Lif medium for another 5 days. Colonies were stained using an Alkaline Phosphatase Assay Kit (System Biosciences) and evaluated under an Olympus CK2 microscope.

#### Embryoid body formation and monolayer differentiation

For embryoid body formation assay,  $3 \times 10^6$  mES cells were seeded into 10 cm bacterial grade Petri dish in 10 ml differentiation medium (DMEM/F12 supplemented with 15% FBS,  $1 \times$  penicillin/streptomycin, 0.1 mM Nonessential Amino Acids, 2 mM L-glutamine, and 50  $\mu$ M 2-mercaptoethanol), and maintained on a horizontal rotator with a rotating speed of 30 rpm. The medium was changed at Day 3 and the resultant EBs were harvested at Day 5. For monolayer differentiation,  $1 \times 10^4$  mES cells per well were seeded into gelatin-coated six-well plates in 2 ml differentiation medium for 2 days.

#### Neural cell differentiation

mESCs were dissociated and seeded onto 10  $\mu$ g/ml laminin-coated six-well plates at a density of  $1 \times 10^4$  cells/cm<sup>2</sup> in N2B27 medium (Mulas et al, 2019). The medium was changed on Day 2 and every day thereafter. Cells were harvested at the indicated time points.

#### Polysome analysis

Polysome analysis was performed using the methods described previously (Zhang et al, 2017). Briefly, mESCs were lysed in the polysome lysis buffer (10 mM Tris-HCl pH 7.4, 12 mM MgCl<sub>2</sub>, 100 mM KCl, 1% Tween-20, and 100 mg/ml cycloheximide). Then, 5 OD260 cell lysate was loaded onto a 5–50% (w/v) linear sucrose-density gradient, followed by centrifugation at 200,000 g in a Beckman SW-41Ti rotor for 2 h at 4°C. The gradient was fractionated using a Gradient Station (BioComp) coupled with an ultraviolet 254 nm detector (Bio-Rad EM-1).

#### CLIP-seq and peak calling, and RNA-seq

CLIP-seq was performed using the method described in the previous paper. The peak calling was performed using the pipeline described previously (Chen et al, 2019; Liu et al, 2021a).

## Data availability

The CLIP-seq and RNA-seq data from this publication have been deposited to the Gene Expression Omnibus (GEO) database (<https://www.ncbi.nlm.nih.gov/geo/>) and assigned the identifiers are GSE183715, respectively.

**Expanded View** for this article is available [online](#).

#### Acknowledgements

This work is supported by Mayo Foundation for Medical Education and Research. We thank Drs. J. Alvarez-Dominguez and G. Riddihough for critical comments.

#### Author contributions

**Qiuying Liu:** Formal analysis; investigation; writing – review and editing.  
**Mariah K Novak:** Investigation; writing – review and editing.  
**Rachel M Pepin:** Investigation; writing – review and editing.  
**Katharine R Maschoff:** Investigation; writing – review and editing.  
**Kailey Worner:** Investigation. **Xiaoli Chen:** Software.  
**Shaojie Zhang:** Software. **Wenqian Hu:** Conceptualization; formal analysis; supervision; funding acquisition; investigation; writing – original draft; project administration; writing – review and editing.

#### Disclosure and competing interests statement

The authors declare that they have no conflict of interest.

## References

- Adamo A, Sese B, Boue S, Castano J, Paramonov I, Barrero MJ, Izpisua Belmonte JC (2011) LSD1 regulates the balance between self-renewal and differentiation in human embryonic stem cells. *Nat Cell Biol* 13: 652–659
- Aeschmann F, Kumari P, Bartake H, Gaidatzis D, Xu L, Ciosk R, Grosshans H (2017) LIN41 post-transcriptionally silences mRNAs by two distinct and position-dependent mechanisms. *Mol Cell* 65: 476–489
- Betschinger J, Nichols J, Dietmann S, Corrin PD, Paddison PJ, Smith A (2013) Exit from pluripotency is gated by intracellular redistribution of the bHLH transcription factor Tfe3. *Cell* 153: 335–347
- Brinegar AE, Cooper TA (2016) Roles for RNA-binding proteins in development and disease. *Brain Res* 1647: 1–8
- Chang HM, Martinez NJ, Thornton JE, Hagan JP, Nguyen KD, Gregory RI (2012) Trim71 cooperates with microRNAs to repress Cdkn1a expression and promote embryonic stem cell proliferation. *Nat Commun* 3: 923
- Chen Y, Yang Y, Wang F, Wan K, Yamane K, Zhang Y, Lei M (2006) Crystal structure of human histone lysine-specific demethylase 1 (LSD1). *Proc Natl Acad Sci USA* 103: 13956–13961
- Chen J, Lai F, Niswander L (2012) The ubiquitin ligase mLin41 temporally promotes neural progenitor cell maintenance through FGF signaling. *Genes Dev* 26: 803–815
- Chen X, Castro SA, Liu Q, Hu W, Zhang S (2019) Practical considerations on performing and analyzing CLIP-seq experiments to identify transcriptomic-wide RNA-protein interactions. *Methods* 155: 49–57
- Connacher RP, Goldstrohm AC (2021) Molecular and biological functions of TRIM-NHL RNA-binding proteins. *Wiley Interdiscip Rev RNA* 12: e1620
- Cuevas E, Rybak-Wolf A, Rohde AM, Nguyen DT, Wulczyn FG (2015) Lin41/Trim71 is essential for mouse development and specifically expressed in postnatal ependymal cells of the brain. *Front Cell Dev Biol* 3: 20

- Darnell RB (2010) HITS-CLIP: panoramic views of protein-RNA regulation in living cells. *Wiley Interdiscip Rev RNA* 1: 266–286
- Di Stefano B, Luo EC, Haggerty C, Aigner S, Charlton J, Brumbaugh J, Ji F, Rabano Jimenez I, Clowers KJ, Huebner AJ et al (2019) The RNA helicase DDX6 controls cellular plasticity by modulating P-body homeostasis. *Cell Stem Cell* 25: 622–638
- Duy PQ, Weise SC, Marini C, Li XJ, Liang D, Dahl PJ, Ma S, Spajic A, Dong W, Juusola J et al (2022) Impaired neurogenesis alters brain biomechanics in a neuroprogenitor-based genetic subtype of congenital hydrocephalus. *Nat Neurosci* 25: 458–473
- Ecsedi M, Grosshans H (2013) LIN-41/TRIM71: emancipation of a miRNA target. *Genes Dev* 27: 581–589
- Foster DJ, Chang HM, Haswell JR, Gregory RI, Slack FJ (2020) TRIM71 binds to IMP1 and is capable of positive and negative regulation of target RNAs. *Cell Cycle* 19: 2314–2326
- Fraser CS, Doudna JA (2007) Structural and mechanistic insights into hepatitis C viral translation initiation. *Nat Rev Microbiol* 5: 29–38
- Furey CG, Choi J, Jin SC, Zeng X, Timberlake AT, Nelson-Williams C, Mansuri MS, Lu Q, Duran D, Panchagnula S et al (2018) De novo mutation in genes regulating neural stem cell fate in human congenital hydrocephalus. *Neuron* 99: e304
- Gebauer F, Schwarzl T, Valcarcel J, Hentze MW (2021) RNA-binding proteins in human genetic disease. *Nat Rev Genet* 22: 185–198
- Glisovic T, Bachorik JL, Yong J, Dreyfuss G (2008) RNA-binding proteins and post-transcriptional gene regulation. *FEBS Lett* 582: 1977–1986
- Hafner M, Katsantoni M, Köster T, Marks J, Mukherjee J, Staiger D, Ule J, Zavolan M (2021) CLIP and complementary methods. *Nat Rev Methods Primers* 1: 20
- Han X, Gui B, Xiong C, Zhao L, Liang J, Sun L, Yang X, Yu W, Si W, Yan R et al (2014) Destabilizing LSD1 by Jade-2 promotes neurogenesis: an antibraking system in neural development. *Mol Cell* 55: 482–494
- Jin SC, Dong W, Kundishora AJ, Panchagnula S, Moreno-De-Luca A, Furey CG, Allocco AA, Walker RL, Nelson-Williams C, Smith H et al (2020) Exome sequencing implicates genetic disruption of prenatal neuro-gliogenesis in sporadic congenital hydrocephalus. *Nat Med* 26: 1754–1765
- Kahle KT, Kulkarni AV, Limbrick DD Jr, Warf BC (2016) Hydrocephalus in children. *Lancet* 387: 788–799
- Kahvejian A, Svitkin YV, Sukarieh R, M'Boutchou MN, Sonenberg N (2005) Mammalian poly(a)-binding protein is a eukaryotic translation initiation factor, which acts via multiple mechanisms. *Genes Dev* 19: 104–113
- Kaya-Okur HS, Wu SJ, Codomo CA, Pledger ES, Bryson TD, Henikoff JG, Ahmad K, Henikoff S (2019) CUT&tag for efficient epigenomic profiling of small samples and single cells. *Nat Commun* 10: 1930
- Kim SA, Zhu J, Yennawar N, Eek P, Tan S (2020) Crystal structure of the LSD1/CoREST histone demethylase bound to its nucleosome substrate. *Mol Cell* 78: 903–914
- Kozub MM, Carr RM, Lomber GL, Fernandez-Zapico ME (2017) LSD1, a double-edged sword, confers dynamic chromatin regulation but commonly promotes aberrant cell growth. *F1000Res* 6: 2016
- Kumari P, Aeschmann F, Gaidatzis D, Keusch JJ, Ghosh P, Neagu A, Pachulska-Wieczorek K, Bujnicki JM, Gut H, Grosshans H et al (2018) Evolutionary plasticity of the NHL domain underlies distinct solutions to RNA recognition. *Nat Commun* 9: 1549
- Lee FCY, Ule J (2018) Advances in CLIP Technologies for Studies of protein-RNA interactions. *Mol Cell* 69: 354–369
- Li XJ, Du ZW, Zarnowska ED, Pankratz M, Hansen LO, Pearce RA, Zhang SC (2005) Specification of motoneurons from human embryonic stem cells. *Nat Biotechnol* 23: 215–221
- Liu Q, Chen X, Novak MK, Zhang S, Hu W (2021a) Repressing Ago2 mRNA translation by Trim71 maintains pluripotency through inhibiting let-7 microRNAs. *eLife* 10: e66288
- Liu Q, Novak MK, Pepin RM, Eich T, Hu W (2021b) microRNA-mediated regulation of microRNA machinery controls cell fate decisions. *eLife* 10: e72289
- Loedige I, Gaidatzis D, Sack R, Meister G, Filipowicz W (2013) The mammalian TRIM-NHL protein TRIM71/LIN-41 is a repressor of mRNA function. *Nucleic Acids Res* 41: 518–532
- Loedige I, Jakob L, Treiber T, Ray D, Stotz M, Treiber N, Hennig J, Cook KB, Morris Q, Hughes TR et al (2015) The crystal structure of the NHL domain in complex with RNA reveals the molecular basis of drosophila brain-tumor-mediated gene regulation. *Cell Rep* 13: 1206–1220
- Lukong KE, Chang KW, Khandjian EW, Richard S (2008) RNA-binding proteins in human genetic disease. *Trends Genet* 24: 416–425
- Maller Schulman BR, Liang X, Stahlhut C, DelConte C, Stefani G, Slack FJ (2008) The let-7 microRNA target gene, Mlin41/Trim71 is required for mouse embryonic survival and neural tube closure. *Cell Cycle* 7: 3935–3942
- Mulas C, Kalkan T, von Meyenn F, Leitch HG, Nichols J, Smith A (2019) Defined conditions for propagation and manipulation of mouse embryonic stem cells. *Development* 146: dev173146
- Perillo B, Tramontano A, Pezone A, Migliaccio A (2020) LSD1: more than demethylation of histone lysine residues. *Exp Mol Med* 52: 1936–1947
- Van Nostrand EL, Pratt GA, Shishkin AA, Gelboin-Burkhart C, Fang MY, Sundararaman B, Blue SM, Nguyen TB, Surka C, Elkins K et al (2016) Robust transcriptome-wide discovery of RNA-binding protein binding sites with enhanced CLIP (eCLIP). *Nat Methods* 13: 508–514
- Van Nostrand EL, Freese P, Pratt GA, Wang X, Wei X, Xiao R, Blue SM, Chen JY, Cody NAL, Dominguez D et al (2020) A large-scale binding and functional map of human RNA-binding proteins. *Nature* 583: 711–719
- Welte T, Tuck AC, Papasaikas P, Carl SH, Flemer M, Knuckles P, Rankova A, Buhler M, Grosshans H (2019) The RNA hairpin binder TRIM71 modulates alternative splicing by repressing MBNL1. *Genes Dev* 33: 1221–1235
- Whyte WA, Bilodeau S, Orlando DA, Hoke HA, Frampton GM, Foster CT, Cowley SM, Young RA (2012) Enhancer decommissioning by LSD1 during embryonic stem cell differentiation. *Nature* 482: 221–225
- Worringer KA, Rand TA, Hayashi Y, Sami S, Takahashi K, Tanabe K, Narita M, Srivastava D, Yamanaka S (2014) The let-7/LIN-41 pathway regulates reprogramming to human induced pluripotent stem cells by controlling expression of prodifferentiation genes. *Cell Stem Cell* 14: 40–52
- Ying QL, Wray J, Nichols J, Batlle-Morera L, Doble B, Woodgett J, Cohen P, Smith A (2008) The ground state of embryonic stem cell self-renewal. *Nature* 453: 519–523
- Zhang X, Chen X, Liu Q, Zhang S, Hu W (2017) Translation repression via modulation of the cytoplasmic poly(a)-binding protein in the inflammatory response. *eLife* 6: e27786